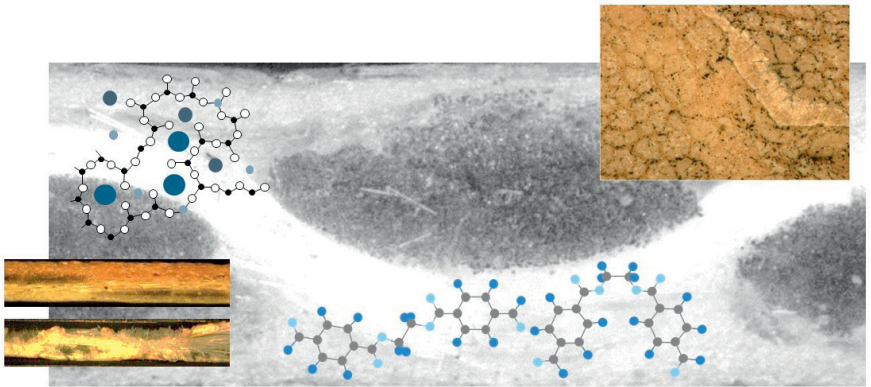


Hastia Asadi



**Strength deterioration of architectural fabrics
under single and combined artificial weathering
impacts**

Strength deterioration of architectural fabrics under single and combined artificial weathering impacts

Von der Fakultät für Ingenieurwissenschaften, Abteilung Bauwissenschaften,
der Universität Duisburg-Essen
zur Erlangung des akademischen Grades

Doktor-Ingenieur

genehmigte Dissertation

von

Hastia Asadi M.Sc.

Referentin: Univ.-Prof. Dr.-Ing. habil. Natalie Stranghöner

Korreferent: Univ.-Prof. Dr. rer. nat. Mathias Ulbricht

Eingereicht: 08. Juni 2021

Mündliche Prüfung: 15. November 2021

Abteilung Bauwissenschaften der Fakultät für Ingenieurwissenschaften

Institut für Metall- und Leichtbau

Univ.-Prof. Dr.-Ing. habil. Natalie Stranghöner

Schriftenreihe Institut für Metall- und Leichtbau
Universität Duisburg-Essen
herausgegeben von
Univ.-Prof. Dr.-Ing. habil. Natalie Stranghöner

Band 9

Hastia Asadi

**Strength deterioration of architectural fabrics under
single and combined artificial weathering impacts**

Shaker Verlag
Düren 2022

Bibliographic information published by the Deutsche Nationalbibliothek

The Deutsche Nationalbibliothek lists this publication in the Deutsche Nationalbibliografie; detailed bibliographic data are available in the Internet at <http://dnb.d-nb.de>.

Zugl.: Duisburg-Essen, Univ., Diss., 2021

Copyright Shaker Verlag 2022

All rights reserved. No part of this publication may be reproduced, stored in a retrieval system, or transmitted, in any form or by any means, electronic, mechanical, photocopying, recording or otherwise, without the prior permission of the publishers.

Printed in Germany.

ISBN 978-3-8440-8562-4

ISSN 1867-6782

Shaker Verlag GmbH • Am Langen Graben 15a • 52353 Düren

Phone: 0049/2421/99011-0 • Telefax: 0049/2421/99011-9

Internet: www.shaker.de • e-mail: info@shaker.de

Abstract

Nowadays, the application of coated fabrics as an architectural membrane material for lightweight structures is growing dramatically. Despite the fact that a lot of research has been carried out on the properties of these fabrics, yet broad assumptions are made in both material testing and modelling of the material behaviour. Under weathering, the degradation of these materials within the coating and its propagation to the fibres contributes to the loss of functional performance, mainly in terms of mechanical properties such as the tensile strength. The durability of the fabrics is also evaluated by the loss in mechanical performance. Till now, verified numbers for factors considering this strength reduction in the framework of either a national or an international standard are missing.

This thesis describes investigations into the uniaxial tensile strength deterioration of two common architectural coated woven fabrics, PET-PVC and glass-PTFE, exposed to various artificial weathering factors, alone or in combination. This survey is structured based on the combination of a review and original exploratory experimental research. The overview is required to provide the fundamental declaration of each layer of architectural fabrics' chemical compositions and their mechanisms of degradation under different weathering impacts.

The experimental investigation includes the evaluation of artificial ageing influences, first on PET reinforced PVC coated fabrics, and second on glass reinforced PTFE coated fabrics. The impact of water attack by two action mechanisms of chemical reactions and swelling-deswelling is assessed on the tensile strength deterioration. In this way, in-plane and out of plane water seepage and freeze-thaw cycles have been carried out to simulate the detrimental presence of humidity due to rain or snow in both normal and cold weathers. Furthermore, the uniaxial tensile strength sensitivity to different artificial weathering impacts has been determined. The chemical and physical changes of uncoated woven PET fabrics, as the load-bearing element of PET-PVC composite, have been traced by Fourier transform infrared spectroscopy and molecular weight measurements to construct a degradation pathway network model for estimation of possible degradation mechanisms.

The additional contribution of this thesis is the set of weathering-induced ageing modification factors derived from the artificial weathering test results in order to broaden the database in the frame of European design standardization.

Kurzfassung

Heutzutage nimmt die Anwendung von beschichteten Geweben als architektonisches Membranmaterial für Leichtbaukonstruktionen enorm zu. Trotz der Tatsache, dass viel über die Eigenschaften dieser Gewebe geforscht wurde, werden sowohl bei der Materialprüfung als auch bei der Modellierung des Materialverhaltens pauschale Annahmen getroffen. Unter Bewitterung trägt die Degradation dieser Materialien innerhalb der Beschichtung und ihre Ausbreitung auf die Fasern zum Verlust der funktionellen Leistung bei, hauptsächlich in Bezug auf die mechanischen Eigenschaften wie die Zugfestigkeit. Die Haltbarkeit der Gewebe wird auch durch den Verlust an mechanischer Leistung bewertet. Bislang fehlen jedoch verifizierte Zahlen für Faktoren, die diese Festigkeitsminderung im Rahmen einer nationalen oder internationalen Norm berücksichtigen.

Diese Arbeit beschreibt die Untersuchung der Abnahme der monoaxialen Zugfestigkeit von zwei gebräuchlichen architektonischen beschichteten Geweben, PET-PVC und Glas-PTFE, die verschiedenen künstlichen Bewitterungsfaktoren, allein oder in Kombination, ausgesetzt sind. Diese Untersuchung ist auf der Grundlage einer Kombination aus einer Literaturliteraturauswertung und -bewertung sowie einer experimentellen Grundlagenuntersuchung aufgebaut. Diese Übersicht dient der grundlegenden Erklärung der chemischen Zusammensetzungen der einzelnen Schichten von Architekturgeweben und ihrer Degradationsmechanismen unter verschiedenen Bewitterungseinflüssen.

Die experimentelle Untersuchung umfasst die Bewertung künstlicher Alterungseinflüsse an PET-verstärkten PVC-beschichteten Geweben und an glasverstärkten PTFE-beschichteten Geweben. Der Einfluss des Wasserangriffs durch die beiden Wirkmechanismen der chemischen Reaktionen und des Quellens-Abschwellens wird auf die Verschlechterung der Zugfestigkeit bewertet. Auf diese Weise sollen das Eindringen von Wasser in der Ebene und außerhalb der Ebene sowie Frost-Tau-Zyklen simuliert werden, um die nachteilige Anwesenheit von Feuchtigkeit durch Regen oder Schnee sowohl bei normalem als auch bei kaltem Wetter zu simulieren. Weiterhin wird die Empfindlichkeit der einachsigen Zugfestigkeit gegenüber verschiedenen künstlichen Bewitterungseinflüssen ermittelt. Die chemischen und physikalischen Veränderungen von unbeschichteten, gewebten PET-Geweben als tragendes Element des PET-PVC-Verbunds werden mittels Fourier-Transformations-Infrarotspektroskopie und Molekulargewichtsmessungen verfolgt, um ein Degradationspfad-Netzwerkmodell zur Abschätzung möglicher Degradationsmechanismen zu konstruieren.

Der zusätzliche Beitrag dieser Arbeit ist die Zusammenstellung von witterungsbedingten Alterungsmodifikationsfaktoren, die aus den Ergebnissen der künstlichen Bewitterungstests abgeleitet wurden, um die Datenbasis als Grundlage für die europäische Bemessungsnormung zu erweitern.

Preface and Acknowledgements

There are many who helped me along the way on this journey. I want to take a moment to thank them.

First, I would like to acknowledge the scholarship provided by University Duisburg-Essen for funding this thesis.

I wish to express appreciation to my advisors Professor Natalie Stranghöner and Professor Mathias Ulbricht for their support and motivation, and to my thesis committee members Professor Doru Lupascu, Professor Renatus Widmann, Professor Eugen Perau for their valuable insights and advice throughout this work. I would like to express my sincere gratitude to Dr. Jörg Uhlemann for his treasured constant support which was really influential in shaping my experimental studies and critiquing my results. Your help was extremely valuable.

I gratefully appreciate all the members of ELLF lab, who have shared and contributed in many ways to make life in the lab easier, especially Stefanie Schülpen, Thomas Homm, Andre Westerhoff, and Kinan Masoud.

Extra thanks are extended to Professor Thomas Schrader, Professor Mathias Ulbricht, and Professor Doru Lupascu who generously shared equipment and expertise and also Dr. Klaus Opwis, Deutsches Textilforschungszentrum Nord-West gGmbH for assistance with Yellowness index measurement.

My sincer thanks go to my friends Maryam Mirjalali, Farnoosh Hedayati, Aida Alehashemi, Amin Tolue, and also my colleagues at Institute for Metal and Lightweight Structures.

I am deeply grateful to my previous advisors, Professor Masoud Mirtaheri and Amir Peyman Zandi at K. N. Toosi University of Technology for all their supports.

I want to thank my family, Zhila Nashat, Mohammad Esmaeil Asadi, Soroush Asadi, and Behsa Asadi, for their endless love and being always there for me offering all kinds of encouragement and understanding.

Finally, to my boyfriend, Christoph Abraham: your love and understanding helped me through this step. It is time to celebrate; you earned this degree right along with me.

In the end, I would like to dedicate this work to all Iranian social activists, journalists, lawyers as well as ordinary people who sacrifice their lives for freedom.

Essen, in November 2021

Content

1	INTRODUCTION	1
1.1	Topic	1
1.2	Motivating questions.....	5
1.3	Objectives and aims	6
1.4	Work plans and risks	6
1.5	Methodical approach.....	7
2	ARCHITECTURAL COATED WOVEN FABRIC, DIFFERENT LAYERS, AND CHEMICAL COMPOSITIONS	9
2.1	General	9
2.2	Polyvinyl chloride-coated woven polyethylene terephthalate fabric (PET-PVC)	11
2.2.1	General.....	11
2.2.2	Polyethylene terephthalate (PET) woven fabric.....	12
2.2.3	Adhesion, Isocyanate compound.....	14
2.2.4	Polyvinyl chloride (PVC) coating.....	15
2.2.5	Primer.....	17
2.2.6	Top coating.....	17
2.3	Polytetrafluoroethylene (PTFE)-coated woven glass fibre fabric (Glass-PTFE)	18
2.3.1	General.....	18
2.3.2	Glass fibre fabric	19
2.3.3	Finish layer as deposited solids on the glass fibre	19
2.3.4	Primer, silicon.....	21
2.3.5	Polytetrafluoroethylene ethylene (PTFE) coating	21
2.4	Tensile properties	23
2.4.1	General.....	23
2.4.2	Definition of the tensile strength in coated woven fabrics	23
2.4.3	Uniaxial strip and grab test methods.....	23
2.4.4	Stress-strain curves	24
2.5	Saturation behaviour under cyclic loading	26
2.6	Discussion and conclusions	28
3	AGEING MECHANISMS	29
3.1	General	29
3.2	Ageing of polymers	29
3.2.1	General.....	29
3.2.2	Physical ageing	29
3.2.3	Chemical ageing	30
3.2.4	Mechanical ageing	30
3.3	Weathering of membrane material	30
3.3.1	General.....	30
3.3.2	Atmospheric oxygen.....	31

3.3.3 Sunlight	32
3.3.4 Heat.....	33
3.3.5 Water or humidity	34
3.3.6 Pollutants.....	37
3.3.7 Microorganism.....	37
3.3.8 Blowing dirt and dust.....	37
3.3.9 Mechanical stress	37
3.4 Weathering of PET-PVC	38
3.4.1 General.....	38
3.4.2 Mechanisms of weathering degradations of PET	39
3.4.3 Effects of exposure on PET degrading	42
3.4.4 Mechanisms of PVC degradation under the influence of different factors	44
3.4.5 Effects of PVC exposure to degradation conditions	45
3.5 Weathering of glass-PTFE.....	45
3.5.1 General.....	45
3.5.2 Change of mechanical properties of glass due to humidity	45
3.5.3 Humidity impact onto other elements of glass-PTFE fabric.....	48
3.6 Characterization of weathered polymers.....	50
3.7 Weathering procedures	50
3.7.1 General.....	50
3.7.2 Natural weathering	50
3.7.3 Natural accelerated weathering	53
3.7.4 Artificial accelerated weathering	53
3.7.5 Artificial light sources	54
3.7.6 Weathering by practical application	54
3.7.7 Correlations between artificial and natural weathering	55
3.7.8 Weathering of PET-PVC and glass-PTFE, state of the art.....	56
3.8 Discussion and conclusions	63
4 EXPERIMENTAL INVESTIGATION: WEATHERING OF PET-PVC AND GLASS-PTFE FABRICS.....	65
4.1 Survey of investigated materials	65
4.1.1 General.....	65
4.1.2 Weathering by practical application	65
4.1.3 Artificial weathering	65
4.2 Exposure condition	68
4.2.1 General.....	68
4.2.2 Weathering by practical application	68
4.2.3 Artificial weathering	69
4.2.4 Water exposure.....	72
4.2.5 Temperature exposure.....	76
4.2.6 Cyclic loading	77
4.3 Analytical method	78
4.3.1 Statistical evaluation	78
4.3.2 Time degradation curves.....	78
4.3.3 Lifetime and Degradation Science approach (L&DS)	78
4.4 Characterization of mechanistic variables and performance level responses.....	79
4.4.1 Uniaxial tensile strength	79
4.4.2 Stiffness.....	80
4.4.3 Infrared spectroscopy.....	81
4.4.4 Yellowness index measurement	82

4.4.5 Intrinsic viscosity and molecular weight measurement.....	83
4.4.6 Optical microscopy.....	85
4.5 Discussion and conclusion	86
5 RESULTS: WEATHERING OF PET-PVC FABRICS.....	87
5.1 Practical application weathering - tensile strength deterioration.....	87
5.2 Water studies - tensile strength deterioration	88
5.2.1 Water diffusion impact.....	88
5.2.2 Freeze-thaw impact.....	95
5.3 Artificial weathering of uncoated and PVC-coated PET woven fabrics	99
5.3.1 General.....	99
5.3.2 Tensile strength deterioration over weathering time.....	100
5.3.3 Uncoated PET woven fabric.....	102
5.3.4 Sensitivity assessment of different weathering factors and cyclic loading- tensile strength changes.....	111
5.3.5 Saturation of the stress-strain behaviours of artificially weathered PET-PVC materials ..	127
5.3.6 Reciprocity principle-tensile strength deterioration	130
5.4 Discussion and conclusions	132
6 RESULTS: WEATHERING OF GLASS-PTFE FABRICS.....	135
6.1 Water studies - tensile strength deterioration	135
6.1.1 General.....	135
6.1.2 Water diffusion impact.....	135
6.1.3 Freeze-thaw impact.....	150
6.2 Artificial weathering of glass-PTFE fabrics.....	157
6.2.1 General.....	157
6.2.2 Sensitivity assessment of different weathering factors and cyclic loading-tensile strength deterioration	158
6.2.3 Discolouration	165
6.2.4 Saturation of the stress-strain behaviour of artificially weathered glass-PTFE materials..	166
6.3 Comparison of the weathering sensitivity of the surveyed PET-PVC with glass-PTFE fabrics	168
6.4 Discussion and conclusions	168
7 WEATHERING-INDUCED AGEING MODIFICATION FACTOR	171
7.1 General	171
7.2 Correlation between natural and artificial weathering	171
7.3 Proposed weathering-induced ageing modification factors, PET-PVC	173
7.3.1 Weathering-induced ageing factor, practical weathering application	173
7.3.2 Deterioration effect by humidity	173
7.3.3 Weathering-induced ageing factor, various artificial weathering methods	173
7.4 Proposed weathering-induced ageing modification factors, glass-PTFE	179
7.4.1 Deterioration effect by humidity	179
7.4.2 Weathering-induced ageing factor, various artificial weathering methods	179

7.5 Discussion and conclusions	190
8 DISCUSSIONS, CONCLUSIONS, AND OUTLOOK.....	191
8.1 General	191
8.2 Experimental investigations	191
8.3 Outlook	192
REFERENCES.....	195
Glossary	209
Annex A: Chronologically tabulated literatures, PET-PVC and glass-PTFE fabrics.....	211
Annex B: Test results, uncoated woven PET and PET-PVC fabrics.....	233
Annex C: Test results, glass-PTFE fabrics.....	259

List of Figures

Figure 1: Different types of tensile structures	1
Figure 2: Possible modes of defects in fabric structures	3
Figure 3: Different kinds of architectural woven fabrics	10
Figure 4: Schematic view of different layers of PET-PVC	11
Figure 5: Cross-section view (cut through weft yarns of a PET-PVC fabric, type IV, see Table 10), Scanning electron microscope method	11
Figure 6: The repeating unit of PET	12
Figure 7: Isomers of PET molecules	14
Figure 8: Chemical structure of PVC	15
Figure 9: Up: thermal degradation of PVC and down: the chemical reaction of mixed metal stabilizer with PVC	17
Figure 10: Chemical structure of polyvinylidene fluoride (PVDF)	18
Figure 11: Schematic view of different layers of glass-PTFE	19
Figure 12: Hydrolysis of typical organosilane and formation of complex multimolecular layer deposit	20
Figure 13: Glass sphere (approximately 17 μm) visible at the rupture line, Glass-PTFE type IV, SEM method	22
Figure 14: Cross-section view of coating irregularities, glass-PTFE type IV, first batch, left: cut through warp yarns; right: cut through weft yarns; SEM method	22
Figure 15: Stress-strain curves of uncoated PET and coated PET-PVC type II	25
Figure 16: Engineering stress-strain curves of glass-PTFE type II	26
Figure 17: Typical stress-strain diagrams for uniaxial testing, illustrate nonlinearity, inelasticity, and anisotropy	27
Figure 18: Weathering factors	30
Figure 19: Hydrocarbon oxidation, RH = polymer, R' = alkyl radical, ROO' = peroxy radical, ROOH = hydroperoxide, RO' = alkoxy, and OH = hydroxyl radical	31
Figure 20: Out of plane water seepage mechanisms through the coated woven fabrics at room temperature	36
Figure 21: Dismantled fabrics taken from two practical applications, left: 23-year-old PET-PVC type III, and right: 38-year-old PET-PVC type II with PVDF top coating	38
Figure 22: Photochemical degradation mechanism	40
Figure 23: Hydrolysis reaction of PET, acidic and basic conditions	41
Figure 24: Thermally activated chain scission of PET	41
Figure 25: Discolouration mechanisms, PET-derived structures	42
Figure 26: Velocity of a running crack versus stress intensity factor	46
Figure 27: Water impact on various elements of glass-PTFE fabric	49
Figure 28: 3D images showing existence of pinholes on the finished surface of glass-PTFE fabrics, up: glass-PTFE type II first batch, down: glass-PTFE type IV first batch, taken by digital optical microscope	50
Figure 29: Natural weathering test rack at UDE-IML/ELLF	52
Figure 30: Artificial weathering, glass-PTFE, state of the art	57
Figure 31: Natural weathering, PET-PVC, state of the art	59
Figure 32: Artificial weathering, PET-PVC, state of the art	60
Figure 33: PET-PVC type III, left: uncoated woven fabric, right: coated woven fabric	68
Figure 34: Artificial weathering chambers at IML/ELLF	70
Figure 35: Technical drawings of test samples	74
Figure 36: Investigated water seepage mechanisms of glass-PTFE specimens	74
Figure 37: Out of plane ink penetration through the coating thickness, left: penetration in the direction of gravity, right: penetration in the opposite direction relative to gravity	75
Figure 38: Left: cold chamber, right up: glass-PTFE surface after freeze cycle, and right down: thaw cycle	76
Figure 39: Heating and drying oven (Mettler) at IML/ELLF	77
Figure 40: 50 kN Zwick/Roell static uniaxial testing machine at IML/ELLF	80
Figure 41: Calculation of E_{secant} for uncoated PET, PET-PVC, and glass-PTFE fabrics	81
Figure 42: IRTracer-100 Shimadzu spectrometer at Institute for Organic Chemistry, University of Duisburg-Essen	82
Figure 43: Inherent viscosity measurement by glass capillary viscometer (Ubbelohde) at 30 $^{\circ}\text{C}$, Lehrstuhl für Technische Chemie II, University of Duisburg-Essen	85
Figure 44: Keyence digital microscope VHX-70 at IML/ELLF	86
Figure 45: Residual tensile strength-aging time curves of projects A and B	87

Figure 46: Micrographs of the PET-PVC type III, project B, images by digital microscope	88
Figure 47: Mean stress-strain curves, dry and watered states according to method WE1-1 of Table 15	90
Figure 48: Mean values of weight, dry and watered states according to method WE1-1 of Table 15	92
Figure 49: Mean values of tensile strength, dry and watered states according to method WE1-1 of Table 15	93
Figure 50: Mean values of E_{secant} , dry and watered states according to method WE1-1 of Table 15 ..	94
Figure 51: Ink penetration through the coating (blue pigments) after six days of watering, PET-PVC type II, cross section view cut through weft yarns	95
Figure 52: Mean stress-strain curves, virgin and freeze-thaw states	96
Figure 53: Weight changes, virgin and freeze-thaw states	97
Figure 54: Relation between water absorption rate and number of freeze-thaw cycles, PET-PVE type II	97
Figure 55: Tensile strength changes, virgin and freeze-thaw states, see more details in Table B7	98
Figure 56: Relation between mean tensile strength and number of freeze-thaw cycles, PET-PVE type II	98
Figure 57: Mean E_{secant} values, virgin and freeze-thaw states, see more details in Table B8	99
Figure 58: Comparison of relation between mean E_{secant} and number of freeze-thaw cycles in PET-PVE type II	99
Figure 59: Mean stress-strain curves of uncoated and PVC-coated PET fabrics type II, cf. Table 9, under different artificial weathering (methods AW4 and AW6-1 and AW7-1) time periods	101
Figure 60: Residual mean tensile strength of uncoated and PVC-coated PET fabrics type II, cf. Table 10, under different artificial weathering time period (methods AW4 and AW6-1 and AW7-1)	102
Figure 61: Changes of chain scission and molecular weight at different artificial weathering duration (method AW4, cf. Table 12), uncoated woven PET type II	103
Figure 62: Tensile strength versus molecular weight, different artificial weathering duration (method AW4, cf. Table 12), uncoated woven PET type II	104
Figure 63: Mean FTIR spectra for virgin and artificially weathered (method AW4, cf. Table 12), uncoated woven PET type II	105
Figure 64: Normalized absorbance changes under artificial weathering condition (method AW4, cf. Table 12)	106
Figure 65: Discolouration under artificial weathering (method AW4, cf. Table 12), left to right: from 0 to 4684 hours in aforementioned steps, uncoated woven PET type II	107
Figure 66: Yellowness index versus exposure time, artificial weathering condition (method AW4, cf. Table 12) from 0 to 4684 h, uncoated woven PET Type II	108
Figure 67: Pathway diagram for the tensile strength deterioration of PET type II under artificial exposure method (method AW4, cf. Table 12), $r =$ Pearson's correlation coefficient, C=O of COOH of carboxylic acid (1688 cm^{-1}), crystallinity ($1343 \text{ cm}^{-1}/1376 \text{ cm}^{-1}$)	109
Figure 68: Direct and multistep pathway diagrams for the tensile strength deterioration of uncoated woven PET type II under artificial exposure (method AW4, cf. Table 12), t: time of exposure and T_s : tensile strength	111
Figure 69: Mean stress-strain curves, weathering techniques (AW1-1, AW2-1, and AW3-1 of Table 12) at temperature $50 \text{ }^\circ\text{C} \pm 3 \text{ K}$, uncoated woven PET type III	112
Figure 70: Mean stress-strain curves, weathering techniques (AW1-2, AW2-2, and AW3-2 of Table 12) at temperature $60 \text{ }^\circ\text{C} \pm 3 \text{ K}$, uncoated woven PET type III	113
Figure 71: Mean stress-strain curves, weathering techniques (AW1-3, AW2-3, and AW3-3 of Table 12) at temperature $70 \text{ }^\circ\text{C} \pm 3 \text{ K}$, uncoated woven PET type III	113
Figure 72: Mean stress-strain curves, weathering techniques (AW1-4, AW2-4, and AW3-4 of Table 12) at temperature $80 \text{ }^\circ\text{C} \pm 3 \text{ K}$, uncoated woven PET type III	114
Figure 73: Mean stress-strain curves, weathering techniques (AW1: UV + temperature + condensation, see Table 12), uncoated woven PET type III	114
Figure 74: Mean stress-strain curves, weathering techniques (AW2: UV + temperature + dark, see Table 12), uncoated woven PET type III	115
Figure 75: Mean stress-strain curves, weathering techniques (AW3: UV + temperature, see Table 12), uncoated woven PET type III	115
Figure 76: Average tensile strength, weathering techniques (AW1, AW2, and AW3 of Table 12), uncoated PET type II	116
Figure 77: Average tensile strength of uncoated woven PET fabric types II and III, artificial weathering technique M1-2 or M4 for 120 hours, cf. Table 12	117
Figure 78: Mean stress-strain curves, various artificial weathering techniques, PET-PVC type II	118

Figure 79: Mean stress-strain curves, various artificial weathering techniques, PET-PVC type IV ...	119
Figure 80: E_{secant} , various artificial weathering techniques, PET-PVC type II.....	120
Figure 81: E_{secant} , various artificial weathering techniques, PET-PVC type IV.....	121
Figure 82: Average tensile strength, various artificial weathering techniques, PET-PVC type II.....	122
Figure 83: Average tensile strength, various artificial weathering techniques, PET-PVC type IV.....	123
Figure 84: Time-degradation curves, PET-PVC type II.....	125
Figure 85: Time-degradation curves, PET-PVC type IV.....	126
Figure 86: Discoloration of PET-PVC fabrics under artificial weathering methods AW6-1 and AW7-1.....	127
Figure 87: Tensile curve of each load pattern (each including 50 load cycles) with the stress amplitude of 3-25 % $f_{m,23}$, PET-PVC type II.....	128
Figure 88: Relationship between cycle number and residual strain after different artificial weathering time periods, methods AW7-2, PET-PVC type II.....	129
Figure 89: Relationship between cycle number and residual strain after different artificial weathering time periods, methods AW7-2, PET-PVC type IV.....	129
Figure 90: Relationship between cycle number and E_{secant} after different artificial weathering time periods, methods AW7-2.....	130
Figure 91: Mean stress-strain curves of uncoated PET type III fabrics under different irradiances with the same cumulative energy (1969.9 kJ/m ²), artificial weathering AW5-1, AW5-2, and AW5-3.....	131
Figure 92: Mean stress-strain curves of PVC-coated woven PET type III fabrics under different irradiances with the same cumulative energy (1969.9 kJ/m ²) artificial weathering AW8-1, AW8-2, and AW8-3.....	132
Figure 93: Mean tensile strength of uncoated (left) and PVC-coated (right) woven PET fabrics type III under different irradiances with the same cumulative energy (1969.9 kJ/m ²).....	132
Figure 94: Mean stress-strain curves of glass-PTFE materials, different watering time periods, method WE1-1.....	136
Figure 95: Stiffness changes of glass-PTFE materials for different watering time periods, method WE1-1.....	137
Figure 96: Weight changes of glass-PTFE materials for different watering time periods.....	138
Figure 97: Change of the tensile strength of glass-PTFE at different watering time periods WE1-1.....	139
Figure 98: Mean stress-strain curves of permanent and temporary states (cf. WE1-1 and WE1-2 of Table 14) at different watering time period glass-PTFE type II, first batch.....	141
Figure 99: Comparison of stiffness, permanent and temporary changes after different periods of watering (cf. WE1-1 and WE1-2 of Table 15), glass-PTFE type II, first batch.....	142
Figure 100: Temporary and permanent changes of the tensile strength after different periods of watering (cf. WE1-1 and WE1-2 of Table 14), glass-PTFE type II, first batch.....	143
Figure 101: Mean stress-strain curves of strip (in-plane + out of plane watering, cf. WE1-1) and tank shaped (out of plane, cf. WE2, WE3-1, and WE3-2 of Table 14) specimens.....	144
Figure 102: Stiffness changes for different watering techniques, cf. WE1-1, WE1-3, WE2, WE3-1, and WE3-2 of Table 14.....	147
Figure 103: Tensile strength changes for different watering techniques, cf. WE1-1, WE1-3, WE2, WE3-1, and WE3-2 of Table 14.....	149
Figure 104: Ink penetration through the coating (blue pigments) after six days of watering (cf. chapter 4.2.4.3), glass-PTFE type IV the first batch, cross section view cut through weft yarns; left: ink penetration in the direction of gravity, right: ink penetration in the opposite direction relative to gravity.....	150
Figure 105: Mean stress-strain curves, virgin and freeze-thaw states, cf. chapter 4.2.4.5.....	151
Figure 106: Comparison of relation between water absorption rate and number of freeze-thaw cycles (cf. chapter 4.2.4.5).....	153
Figure 107: Tensile strength changes, virgin and freeze-thaw states (cf. chapter 4.2.4.5), up: warp and down: weft direction.....	154
Figure 108: Comparison of relation between mean tensile strength and number of freeze-thaw cycles (cf. chapter 4.2.4.5), left: 100 % = virgin dry state, right: 100 % = watered samples for 30 days.....	155
Figure 109: Comparison of relation between mean E_{secant} and number of freeze-thaw cycles (cf. chapter 4.2.4.5).....	156
Figure 110: E_{secant} changes, virgin and freeze-thaw states (cf. chapter 4.2.4.5).....	157
Figure 111: Mean stress-strain curves, various artificial weathering techniques of Table 14, glass-PTFE type II, first batch.....	159
Figure 112: Mean stress-strain curves, various artificial weathering techniques of Table 14, glass-PTFE type III, first batch.....	159

Figure 113: Mean stress-strain curves, various artificial weathering techniques, glass-PTFE type III, third batch	160
Figure 114: E_{secant} , various artificial weathering techniques, glass-PTFE type II, first batch, up: warp direction, and down: weft direction.....	161
Figure 115: E_{secant} , various artificial weathering techniques, glass-PTFE type III, first batch, up: warp direction, and down: weft direction.....	161
Figure 116: E_{secant} , various artificial weathering techniques, glass-PTFE type III, third batch, up: warp direction, and down: weft direction.....	162
Figure 117: Average tensile strength, various artificial weathering techniques, glass-PTFE type II, first batch, up: warp direction, and down: weft direction	164
Figure 118: Average tensile strength, various artificial weathering techniques, glass-PTFE type III, first batch, up: warp direction, and down: weft direction.....	165
Figure 119: Average tensile strength, various artificial weathering techniques, glass-PTFE type III, third batch, up: warp direction, and down: weft direction.....	165
Figure 120: Discoloration of glass-PTFE fabrics, artificial weathering methods AW6-1	166
Figure 121: Cyclic tensile curves with the stress amplitude of 3-25 % $f_{m,23}$, virgin glass-PTFE type III, third batch	166
Figure 122: Relationship between cycle number and residual strain after different artificial ageing time period, methods AW6-2, glass-PTFE type III, third batch, left: warp direction and right: weft direction	167
Figure 123: Relationship between cycle number and E_{secant} after different artificial ageing time period, methods AW6-2, glass-PTFE type III, third batch, left: warp direction and right: weft direction.....	168
Figure 124: Weathering-induced ageing modification factor, investigated PET-PVC types II and IV materials.....	174
Figure 125: Weathering-induced ageing modification factor, investigated glass-PTFE types II, III, and IV materials	180

List of Tables

Table 1: Pros and cons of tension membrane structures	2
Table 2: Different modification factors	4
Table 3: Additives in flexible PVC compounds	17
Table 4: Comparison of the strip and the grab test procedure according to EN ISO 1421	24
Table 5: Natural weathering sites all around the world	52
Table 6: Weathering-induced ageing modification factor of PET-PVC fabrics, state of the art	61
Table 7: Weathering-induced ageing modification factor of glass-PTFE fabrics, state of the art	62
Table 8: Material properties, project A and B	65
Table 9: Standard used for quantification of material properties	65
Table 10: Summary of all measured and recorded material properties	67
Table 11: Chemical composition of investigated materials	68
Table 12: General features of two real projects	69
Table 13: Artificial weathering cycles of woven uncoated PET membrane material	71
Table 14: Artificial weathering cycles of PET-PVC and glass-PTFE membrane materials	72
Table 15: Different methods of water exposure	75
Table 16: Hysteresis load cycles implemented in AW6-2 and AW7-2, cf. Table 13 and Table 14	77
Table 17: Absorption peaks of polyethylene-terephthalate (PET)	83
Table 18: Direct (cf. Figure 68) and multi-step pathway equations for the tensile strength deterioration of PET type II under artificial exposure (method AW4, cf. Table 12), t: time of exposure (hour), Ts: tensile strength, Cs: chain scission, and Cr: crystallinity	110
Table 19: Changes of E_{secant} values (weathered to virgin state), PET-PVC fabric, different artificial weathering techniques	121
Table 20: Changes of tensile strength (weathered to virgin state), PET-PVC fabrics, different artificial weathering techniques	124
Table 21: Residual tensile strength of glass-PTFE after different watering time periods, method WE1-1	140
Table 22: Magnitude of the tensile strength recovery for glass-PTFE type II after different watering time periods, methods WE1-1 and WE1-2 of Table 15	144
Table 23: Residual tensile strength of glass-PTFE for different water seepage mechanisms	148
Table 24: Residual tensile strength of glass-PTFE, 100 freeze-thaw cycles	154
Table 25: Changes of E_{secant} , 100 freeze-thaw cycles	156
Table 26: Changes of E_{secant} values (weathered to virgin state), glass-PTFE fabric, different artificial weathering techniques	162
Table 27: Changes of tensile strength (weathered to virgin state), glass-PTFE fabrics, different artificial weathering techniques	163
Table 28: Mean annual radiant exposure of two famous geographical benchmark	172
Table 29: Weathering-induced ageing modification factor, Practical application weathering projects, PET-PVC fabric, warp direction, project B	175
Table 30: Weathering-induced ageing modification factor, Practical application weathering projects, PET-PVC fabric, weft direction, projects A and B	176
Table 31: Weathering-induced ageing modification factor, artificial weathering, PET-PVC fabric, warp direction	177
Table 32: Weathering-induced ageing modification factor, artificial weathering, PET-PVC fabric, weft direction	178
Table 33: Watering-induced ageing modification factor, artificial weathering, glass-PTFE fabric, warp direction	181
Table 34: Watering-induced ageing modification factor, artificial weathering, glass-PTFE fabric, weft direction	185
Table 35: Weathering-induced ageing modification factor, artificial weathering, glass-PTFE fabric, warp direction	189
Table 36: Weathering-induced ageing modification factor, artificial weathering, glass-PTFE fabric, weft direction	189

Symbols

Latin

f_{Ed}	the design membrane stress in the considered direction.
f_{Rd}	the design tensile strength of the membrane or the joint related to specific design situation
$f_{k,23}$	the 5 % fractile values of the short-term tensile strength at room temperature (23 °C)
$f_{k,23,virgin}$	the 5 % fractile values of the short-term tensile strength at room temperature (23 °C), virgin dry state
$f_{k,23,watered}$	the 5 % fractile values of the short-term tensile strength at room temperature (23 °C), watered state
k_i	modification factor based on prCEN/TS 19102:2020-10.
A_i	modification factor based on Sap report.
n_{23}	the short-term tensile strength at room temperature (23 °C) in virgin state
$n_{23,w}$	the short-term tensile strength at room temperature (23 °C) in weathered states
E	radiant energy of a photon
h	Plank's constant (6.62×10^{-34} Js)
c	velocity of light (3×10^8 m/s)
I	radiant intensity
t	the exposure time and the flow time
P	Schwarzschild coefficient
T_g	glass-transition temperature
x_i	individual value of a series with n specimens
$f_{m,23}$	mean value of the test results for n tests
V_x	coefficient of variation
S	stressor
M	system-level mechanistic response
R	performance level response
r	Pearson's correlation coefficient
M_w	the average molecular weight
M_n	number average molecular weight
W_i	weight fraction of a polymer chain
M_{wi}	molecular weight of each individual polymer chain
X_i	mole fraction of each individual polymer chain length
w_a	water absorption rate
w_d	initial weight (dry state)
w_w	watered weight

Greek

γ_M	partial factor for resistance
γ_{M0}	partial factor for resistance of material
γ_{M1}	partial factor for resistance of joints
ν	frequency
α	effective UV radiation coefficient
η	intrinsic viscosity
η_r	relative viscosity
η_{inh}	inherent viscosity

Indexes**Latin**

k	characteristic value
m	mean value

Numerical

23	room temperature 23°C
Virgin	virgin state
Watered	watered state

Abbreviations

ULM	ultimate limit state
PES	polyester
PET	polyethylene terephthalate
PVC	polyvinylchloride
BHET	bis(2-Hydroxyethyl) terephthalate
TPA	terephthalic acid
EG	ethylene glycol
DMT	dimethyl terephthalate
IUPAC	international union of pure and applied chemistry
PVDF	polyvinylidene fluoride
PVF	polyvinyl fluoride
PTFE	polytetrafluoroethylene
FEP	fluoroethylene propylene
UV	ultraviolet
SPD	spectral power distribution
AW	artificial weathering
WE	water exposure
SD	standard deviation
COV	coefficient of variation
L&DS	lifetime and degradation science approach
FTIR	Fourier-transform infrared spectroscopy